PAPER • OPEN ACCESS

Study on the influence of orthotropy and tension–compression asymmetry of metal sheets in springback and formability predictions

To cite this article: P.D. Barros *et al* 2018 *J. Phys.: Conf. Ser.* **1063** 012053

View the article online for updates and enhancements.

IOP ebooks™

Bringing you innovative digital publishing with leading voices to create your essential collection of books in STEM research.

Start exploring the collection - download the first chapter of every title for free.

Study on the influence of orthotropy and tension–compression asymmetry of metal sheets in springback and formability predictions

P.D. Barros[1], D.M. Neto[1], J.L. Alves[2], M.C. Oliveira[1], L.F. Menezes[1]

[1] CEMMPRE, Department of Mechanical Engineering, University of Coimbra, Polo II, Rua Luís Reis Santos, 3030-788 Coimbra, Portugal
[2] CMEMS, Department of Mechanical Engineering, University of Minho, Campus de Azurém, 4800-058 Guimarães, Portugal

E-mail: marta.oliveira@dem.uc.pt

Abstract. Most yield criteria possess a point-symmetry with respect to its center, meaning that a stress state and its reverse state have the same absolute value. However, this can be an unrealistic approximation, even for cubic metals (both face-centered cubic and body center cubic)), which can present a small asymmetry between the yield stress in tension and compression, i.e. a strength differential (SD) effect. This work analyzes the influence of taking or not into account the SD effect in the modeling of the sheet orthotropic behavior in the numerical simulation of a cylindrical cup drawing process. The yield criterion adopted is the CPB06 [1], including its version with two linear transformations [2], allowing a better fitting of the experimental data available. The material analyzed presents a quite small tension-compression ratio of 0.963. However, this small SD effect leads to a slightly higher punch force during the bending dominated stage, resulting in a very small influence on the springback prediction. The influence on the thickness evolution during the process is negligible.

1. Introduction

The cylindrical cup forming is commonly used to evaluate the performance of constitutive models, particularly yield criteria. In fact, it is consensual that the earing profile and the thickness distribution obtained in cylindrical cup's forming is dictated by the in-plane distribution of both the r-values and yield stresses, under compression stress states [3]. Unfortunately, the uniaxial in-plane compression test on metal sheets presents some difficulties and, consequently, allow the r-values estimation only for small plastic deformations. Nevertheless, it is possible to evaluate the SD effect using, for instance, the biaxial tension test [4]. Cubic metals are known to present a small SD effect, which gives rise to the question on how important it is to take it into account in the yield criterion adopted in the numerical simulation of a cylindrical cup drawing process.

This work analyses the influence of the SD effect on the prediction of the springback and the strain evolution during the forming of a cup. The example selected is the "BENCHMARK 2 – Cup Drawing of Anisotropic Thick Steel Sheet", proposed under the NUMISHEET 2018 conference. This example is briefly described in section 2, comprising also the details concerning the finite element model adopted. The yield criterion developed by Cazacu et al. 2006 (CPB06) [1] is selected, including its formulation with two linear transformations (CPB06ex2) [2]. The anisotropy parameters of the CPB06ex2 are identified, including or not the SD effect. In order to try to separate the influence of the SD effect from

the orthotropic behavior of the material, the isotropic version of CPB06 yield criterion is also considered, including or not the SD effect. The details concerning the anisotropy parameters identification procedure are also given in section 2. Section 3 presents the results and their discussion. The main conclusions are summarized in section 4.

2. Cup drawing of anisotropic thick steel sheet

The example considered is the deep-drawing and embossing of a hot rolled steel sheet (2.8 mm thickness) with a tensile strength of 440 MPa (SAPH 440 in Japanese Industrial Standard), as schematically shown in Figure 1. This corresponds to the conditions specified for the task that involves the evaluation of the die height at which the blank fractures at the apex of the center boss, but it will be used in this study also to evaluate the influence of the constitutive model in the springback prediction. The stripper applies a force of 50 kN to the blank, which is kept constant during the operation using knockout cylinders. The blank has an initial diameter of 246 mm.
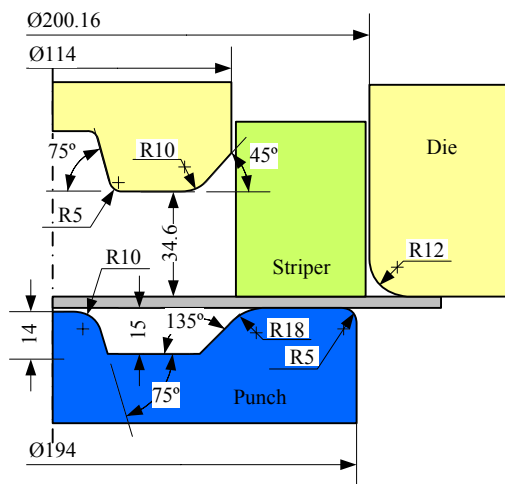

Figure 1. Schematic illustration of the tools geometry and specimen used in the cup drawing test. All dimensions are in millimeter.
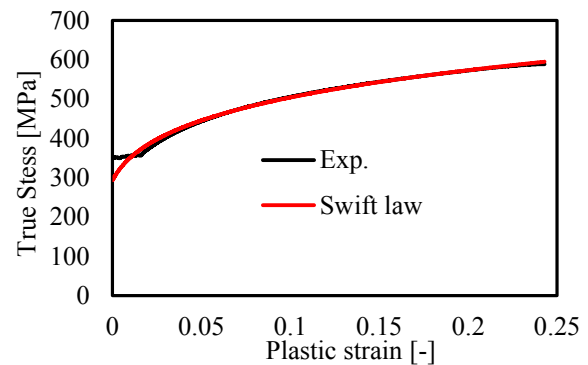
Figure 2. True stress–plastic strain curve of the SAPH 440 steel sheet and hardening law fitted from the uniaxial tensile test in the rolling direction (RD).

2.1. Finite element model

All numerical simulations were performed with the in-house finite element code DD3IMP [5], assuming that the forming tools are rigid and described with Nagata patches [6]. The Coulomb friction law is adopted considering a constant value for the friction coefficient of 0.15, as recommended by the benchmark committee. Only one-quarter model is simulated, allowing to perform the discretization of the blank with 60552 hexahedral finite elements (4 layers through the thickness), using selective reduced integration. The RD is initially aligned with the Ox-axis.

The plastic behavior of the steel sheet (SAPH 440) is described by the isotropic work hardening (Swift law). The stress–strain curve obtained from the uniaxial tensile test, performed along the rolling direction (RD), is used to fit the parameters of the Swift law, as shown in Figure 2.

2.1.1. Yield criteria.
The CPB06 yield criterion allows the description of both the orthotropic behavior and the strength-differential (SD) effect, i.e. tension-compression asymmetry. The equivalent stress $\bar{\sigma}$ associated with its orthotropic form is defined as

$$\bar{\sigma} = B\left[\left(|s_1| - k\, s_1 \right)^a + \left(|s_2| - k\, s_2 \right)^a + \left(|s_3| - k\, s_3 \right)^a \right]^{\frac{1}{a}},$$ (1)

where the exponent a (positive integer) and k are material parameters and the eigenvalues of the tensor $\mathbf{s}$ are denoted by s_1, s_2 and s_3. The tensor $\mathbf{s}$ is determined following a linear transformation, such that $\mathbf{s} = \mathbf{C} : \boldsymbol{\sigma}'$, where $\boldsymbol{\sigma}'$ is the deviatoric stress tensor and $\mathbf{C}$ is the constant 4th-order transformation tensor, defining the 9 anisotropy coefficients. B is a constant defined such that $\bar{\sigma}$ reduces to the tensile yield stress in the RD.

The adoption of a single linear transformation may limit the proper description of both the yield stress and r-values in-plane directionalities. Therefore, the CPB06 was extended to consider two linear transformations of the deviatoric stress tensor [2], i.e. another constant 4th-order transformation tensor, $\mathbf{C}'$, and a k' are considered. The convexity is guaranteed for a≥2 and k and $k' \in [-1,1]$, since the use of one or several linear transformation does not affect convexity of the yield function. For $\mathbf{C}=\mathbf{C}'$ and $k=k'$, the CPB06ex2 yield criterion reduces to the original form of the CPB06. When considering metallic sheets, the anisotropy parameters C_{44}, C'_{44}, C_{55} and C'_{55}, cannot be evaluated. Thus, the corresponding isotropic values are adopted, i.e. 1.0. Moreover, the C_{11} and C'_{11} parameters are also considered equal to 1.0 to avoid equivalent sets of parameters, as discussed in [7]. Therefore, it is necessary to identify a total of 12 anisotropy parameters, both k and k' values and the exponent a.

2.1.2. Material parameters identification. The anisotropy parameters of the CPB06ex2 yield criterion were identified using the DD3MAT in-house code [8]. The procedure adopted is based on the minimization of an error function, evaluating the difference between estimated and experimental values [9]. The experimental values considered were the yield stress and r-values in-plane directionalities and the r_b and the equibiaxial stress σ_b. When considering also the SD effect, the ratio between tensile (σ^{T}) and compressive (σ^{C}) yield stresses, at the RD and the transverse direction (TD), were also used. Since there is no information regarding the compression r-values, their in-plane evolution was carefully monitored and taken into account when selecting the a value in order to avoid odd evolutions or even no physical meaning (e.g. $r<0$ [10]).
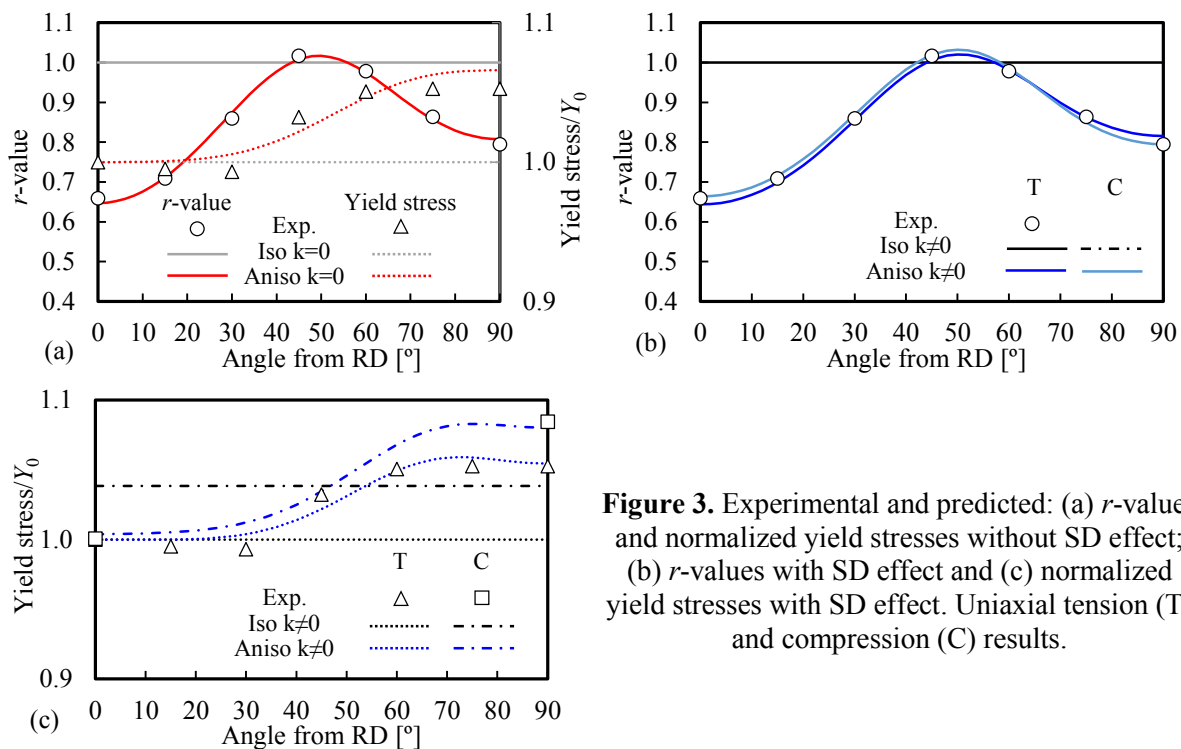

Figure 3. Experimental and predicted: (a) r-values and normalized yield stresses without SD effect; (b) r-values with SD effect and (c) normalized yield stresses with SD effect. Uniaxial tension (T) and compression (C) results.

Figure 3 presents the comparison between the experimental and predicted in-plane distributions of the *r*-values and yield stresses. The trend presented for the experimental normalized yield stress values was evaluated neglecting the initial plateau (see Figure 2). The proper definition of the in-plane directionalities and the biaxial values (see Table 1) is obtained for the CPB06ex2 with *a*=3, taking (Aniso_k=0) or not (Aniso_k≠0) the SD effect into account. In order to try to evaluate only the impact of the SD effect, the CPB06 yield criterion was also used, considering the same value of *a*=3, with (Iso_k=0) or without (Iso_k≠0) the SD effect. In this last case, the *k* value was identified considering the highest $\sigma^{\mathrm{T}}/\sigma^{\mathrm{C}}$ ratio reported experimentally at $\varepsilon_0^{\mathrm{p}}$ =0.01, which corresponds to the TD direction, i.e. $\sigma_{\mathrm{TD}}^{\mathrm{T}}/\sigma_{\mathrm{TD}}^{\mathrm{C}}$ =0.9630, leading to *k*=-0.0315 [1]. Figure 4 presents the yield surfaces predicted for both yield criteria. Note that the Iso_k≠0 leads to the same tension-compression stress ratio for the three axis of 0.9630, while the Aniso_k≠0 leads to: $\sigma_{\mathrm{RD}}^{\mathrm{T}}/\sigma_{\mathrm{RD}}^{\mathrm{C}}$ =0.9962; $\sigma_{\mathrm{TD}}^{\mathrm{T}}/\sigma_{\mathrm{TD}}^{\mathrm{C}}$ =0.9762 and $\sigma_{\mathrm{ND}}^{\mathrm{T}}/\sigma_{\mathrm{ND}}^{\mathrm{C}}$ =0.9942.

Table 1. Identified parameters for the SAPH 440 steel ($C_{11}=C_{44}=C_{55}=C'_{11}=C'_{44}=C'_{55}=1.0$) and predicted r_b (experimental: 0.6390) and normalized equibiaxial stress σ_b (experimental: 1.0200).

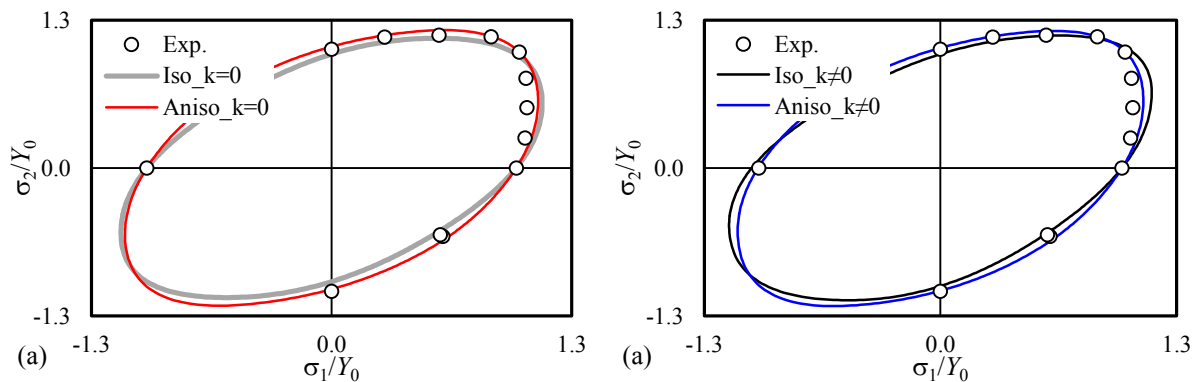|	C_{22}	C_{33}	C_{66}	C_{23}	C_{13}	C_{12}	k'	r_b	σ_b/Y_0
Aniso_k=0	1.0901	-0.9745	-1.2075	0.3527	-0.1806	0.0327	0.0		
	C'_{22}	C'_{33}	C'_{66}	C'_{23}	C'_{13}	C'_{12}	k'	0.6453	1.0176
	1.1796	0.9892	-0.9232	0.1350	-0.22194	0.1032	0.0		
	C_{22}	C_{33}	C_{66}	C_{23}	C_{13}	C_{12}	k'	r_b	σ_b/Y_0
Aniso_k≠0	0.7376	-1.0855	-1.1613	0.2626	-0.2179	0.0271	-0.0009		
	C'_{22}	C'_{33}	C'_{66}	C'_{23}	C'_{13}	C'_{12}	k'	0.6515	1.0184
	1.3604	1.0415	1.0112	0.2037	-0.1871	0.0703	-0.0191		

Figure 4. Normalized yield surfaces predicted by both yield criteria in the $\sigma_1 - \sigma_2$ plane (with $\sigma_3 = 0$) including experimental values at $\varepsilon_0^{\mathrm{p}}$ =0.01: (a) without SD effect; (b) with SD effect.

3. Results and discussion

Figure 5 (a) presents the predicted die force evolution using the different identifications, highlighting the different stages of the forming process. The force increases until approximately 18 mm of die displacement as a result of the bending of the blank flange over the punch radius. Afterward, the force decreases but presents some oscillations, which can be related with the contact conditions, i.e. the frequency is related with the in-plane radial dimension of the finite element mesh adopted. During the bending process, the unsupported flange develops some wrinkles, as shown in Figure 5 (b) for 25 mm of die displacement. After a die displacement of approximately 35 mm, the force starts to increase again, due to the start of the embossing process. The increasing trend is also a result of the thickening of the unsupported flange during the bending process, particularly in the region that presents no contact with the tools. As shown in Figure 6 (a), for a die displacement of 40 mm, there are regions in the unsupported

flange with a thickness higher than the gap between the punch and the die, which is 3.08 mm (see Figure 1). This means that some ironing will occur.

Globally, all models predict a similar die force evolution, except in the stage which involves the ironing of the unsupported flange, as a result of the higher thickening predicted by the models that describe the orthotropic behavior of the blank (see Figure 6 (a)). Considering isotropic plastic behavior, the die force evolution is slightly higher for the model that takes into account the SD effect, which is in agreement with the small increase of the compressive yield stress. This justifies the slightly higher radial coordinate of the inner surface of the cup wall (see Figure 5 (b)), since it becomes slightly harder to bend the material over the punch shoulder radius. Figure 6 (a) shows that the thickness is sensible to the model adopted, particularly to the description of the material orthotropic behavior. However, the evolution of the predicted thickness at the apex of the center boss is similar for all models (see Figure 6 (b)) The analysis of the thickness evolution was performed until a thinning of approximately 50%, i.e. a total displacement of 47 mm was imposed to the die (see Figure 5 (a)).
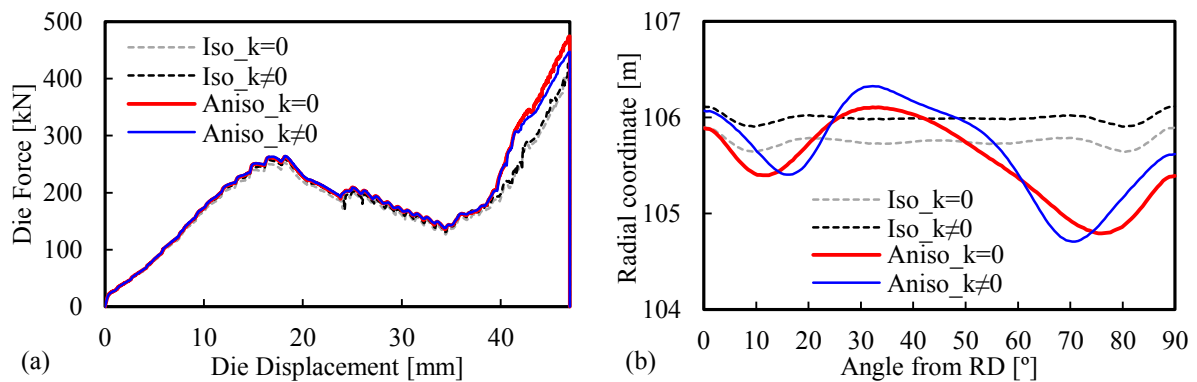

Figure 5. Influence of the yield criterion in the predicted: (a) die force evolution and (b) radial coordinate of the inner surface of the cup wall, for a die displacement of 25 mm.
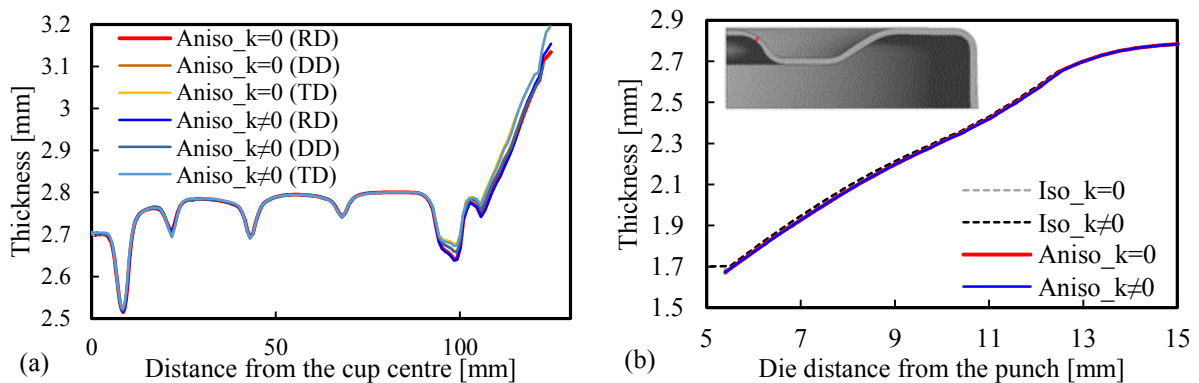

Figure 6. Predicted thickness: (a) distribution along the RD, DD and TD with CPB06ex2, for a die displacement of 40 mm; and (b) evolution at the apex of the center boss, in function of the distance between the die and the bottom dead center of the punch.

Figure 7 (a) presents a detail of the inner surface of the cup along the RD, after a die displacement of 25 mm and springback. For this die displacement, the center boss of the punch has no contact with the blank. The springback mainly changes the geometry of the parts bottom, which becomes less flat. This behavior is identical for all models since the through-thickness distribution of the stress component along the RD in the material frame is also similar, as shown in Figure 7 (b) for the profile located in the Ox-Oz plane. The range of this stress component is mainly dictated by the fact that the model takes or not into account the orthotropic behavior of the material, i.e. the SD effect is small.
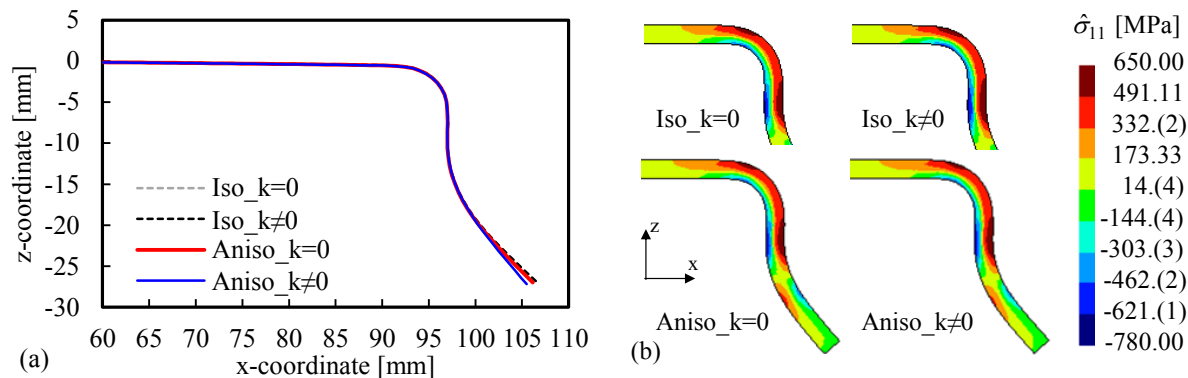
Figure 7. Influence of the yield criterion in the predicted: (a) profile after springback and (b) stress component along the RD in the material frame, for a die displacement of 25 mm.

4. Conclusions

The influence of considering a small SD effect in the numerical simulation of a cylindrical cup deep drawing process is studied. The material selected is a SAPH 440 hot rolled steel that presents a quite small tension-compression ratio of 0.963. This SD effect is modeled considering isotropic behavior, using the CPB06 yield criterion. Moreover, both the orthotropic behavior and the SD effect are described by the CPB06ex2 yield criterion. It is known that the tension-compression asymmetry can influence the neutral line position in bending dominated processes and, consequently, the strain distribution [7] and springback. Nevertheless, for the part under analysis, the influence of both the orthotropic behavior and the SD effect on the predicted springback is small. The thickness distribution in the initially unsupported flange of the part is mainly controlled by the orthotropic behavior of the material, but it has a negligible effect at the apex of the center boss. This work assumed an equal in-plane distribution of the *r*-values for both uniaxial tension and compression stress states, in the identification of the CPB06ex2 yield criterion parameters. This aspect should be further studied in future works, which requires improved experimental procedures for evaluation of the compression *r*-values.

Acknowledgments

References

[1]   Cazacu O, Plunkett B and Barlat F 2006 *Int. J. Plast.* **22** 1171–1194
[2]   Plunkett B, Cazacu O and Barlat F 2008 *Int. J. Plast.* **24** 847–866
[3]   Yoon J W, Dick R E and Barlat F 2011 *Int. J. Plast.* **27** 1165–1184
[4]   Hanabusa Y, Takizawa H and Kuwabara T 2010 *Steel Research Int.* **81** 1376-1379
[5]   Menezes L F and Teodosiu C 2000 *J. Mater. Process. Technol.* **97** 100–6
[6]   Neto D M, Oliveira M C and Menezes L F 2017 *Arch. Comput. Methods Eng.* **24** 37–87
[7]   Barros P D, Alves J L, Oliveira MC and Menezes L F 2016 *Int. J. Mech. Sci.* **114** 217–232
[8]   Barros P D, Carvalho P D, Alves J L, Oliveira M C and Menezes L F 2016 *J. Phys. Conf. Ser.* **734**
[9]   Banabic D, Aretz H, Comsa D S and Paraianu L 2005 *Int. J. Plast.* **21** 493–512
[10] Raemy C, Manopulo N and Hora P 2017 *Int. J. Plast.* **91** 182–204